Chapter 18
Structural Complexity in Structural Health Monitoring: Preliminary Experimental Modal Testing and Analysis

Craig J. L. Cowled, David P. Thambiratnam, Tommy H. T. Chan and Andy C. C. Tan

Abstract Many researchers in the field of civil structural health monitoring have developed and tested their methods on simple to moderately complex laboratory structures such as beams, plates, frames, and trusses. Field work has also been conducted by many researchers and practitioners on more complex operating bridges. Most laboratory structures do not adequately replicate the complexity of truss bridges. This paper presents some preliminary results of experimental modal testing and analysis of the bridge model presented in the companion paper, using the peak picking method, and compares these results with those of a simple numerical model of the structure. Three dominant modes of vibration were experimentally identified under 15 Hz. The mode shapes and order of the modes matched those of the numerical model; however, the frequencies did not match.

18.1 Introduction

This paper presents the preliminary modal testing of the structurally complex QUT Benchmark Structure (see Fig. 18.1), which was designed and constructed in response to an identified need to conduct structural health monitoring research on more complex structures, as argued in the companion paper [1].

The numerical model of the structure is described. The aim of the experiment is presented. The equipment is listed, and the test method is detailed. Data are analyzed, and results are presented and discussed. The paper concludes with a discussion of the results that ties in with the aim of the experiment.

C. J. L. Cowled (✉) · D. P. Thambiratnam · T. H. T. Chan · A. C. C. Tan
Queensland University of Technology, 2 George Street, Brisbane, QLD 4001, Australia
e-mail: craig.cowled@qut.edu.au

W. B. Lee et al. (eds.), *Proceedings of the 7th World Congress on Engineering Asset Management (WCEAM 2012)*, Lecture Notes in Mechanical Engineering,
DOI: 10.1007/978-3-319-06966-1_18,

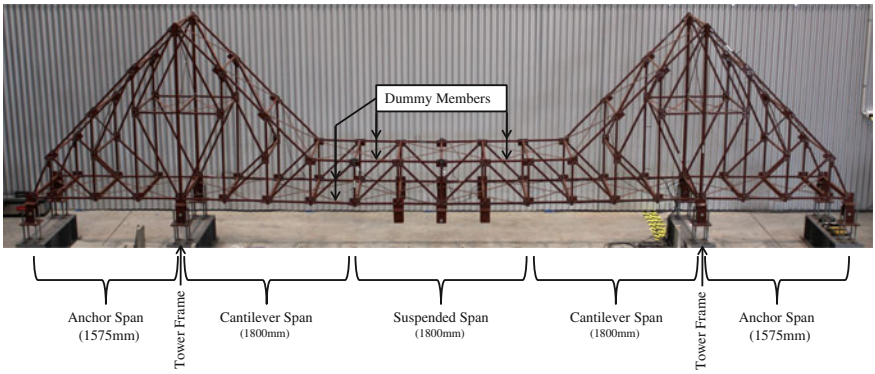

Fig. 18.1 The QUT Benchmark structure

18.2 Preliminary Numerical Model

Two numerical models have been developed for this structure. The first model was developed in Microstran [2] for the purpose of determining the design actions. A second model of the structure has been developed for model updating and damage detection [3]; however, the simple Microstran model is the focus of this paper.

The superstructure was modeled in Microstran as a space frame using the material specifications detailed by Cowled et al. [1]; however, the substructure was not modeled for this preliminary numerical model. The boundary conditions at the base of the tower frames were treated as simple pins, whereas the boundary conditions at the anchor tie down points were treated as rollers. All cross-bracing members were treated as tension only members with pinned joints. Likewise, struts and deck beams were given pinned joints. The fully welded 'H'-shaped tower frames were modeled as members with fully fixed joints. The joints of the chords and webs of the two main trusses were given semi-rigid connections (for in-plane bending), with a rotational stiffness of 10 kNm/rad (value determined by trial and error). The dummy chord members (shown in Fig. 18.1) were given a translational spring of zero stiffness at one end to mimic the slotted-hole structural detail.

The results of the dynamic analysis of the numerical model are presented in Table 18.2 along with those of the preliminary experimental modal analysis.

18.3 Preliminary Test

18.3.1 Aim

The aim of this experiment is to identify, from impact hammer tests, the frequencies, damping, and mode shapes of the first few modes of vibration and compare these results with those from the numerical model of the structure.

18.3.2 Equipment

A list of the equipment used in this experiment is shown in Table 18.1. The data acquisition software used in this experiment was LabVIEW Signal Express 2011 v.5.0.0 [4]. The software used for analysis was MATLAB R2012a [5].

18.3.3 Method

Experimental modal analysis with impact as the excitation force [6] has been adopted as the test method.

Eighteen of the sensors were fixed to the structure. These sensors were located at (or near) twelve node points on the structure with four sensors aligned in the global x direction (longitudinal), eight sensors aligned in the global y direction (vertical), and six sensors aligned in the global z direction (lateral). One sensor was positioned on the bottom flange of one of the 310UC plinth beams to monitor ambient vibrations transmitted to the structure from the concrete slab. Data from the reference sensor were qualitatively scrutinized prior to saving the results of a test. Tests with too much ambient vibration from the reference sensor were rejected and retested.

In order to capture sufficient spatial resolution in the modal model, 65 node points, out of a possible 100, were selected as excitation locations on the structure. A total of 102 impact hammer tests were conducted, representing 102 degrees of freedom (DOFs), of which 20 were aligned in the longitudinal direction, 46 were aligned in the vertical direction, and 36 were aligned in the lateral direction.

In order to capture sufficient resolution in the impact signal, which typically had a duration of 10 ms (based on a few test runs), a sampling frequency of 5.12 kHz was chosen.

Prior to conducting the tests, all machinery in the building, such as the air compressor, water cooler, and fridge, was turned off in an attempt to reduce the influence of ambient vibrations on the test data. In addition to the DOF of the impact, the date, time, air temperature, and relative humidity were recorded.

Each of the 102 tests was repeated at least twelve times. Prior to saving test data, the signals were examined for evidence of double impacts, poorly executed impacts, overshocked sensors, and ‘out of range’ accelerometer readings. Individual repeat tests which failed any one of these criteria were rejected and, if necessary, repeated. The minimum number of successful repeat tests in an impact test was seven, and the maximum number was sixteen.

The raw data from LabVIEW Signal Express [4] were exported to .txt files for transfer to MATLAB [5], where the results were analyzed.

Table 18.1 Experimental equipment

Item description	Qty	Specifications/comments
PCB Piezotronics ICB 086C03 impulse force hammer	1	Range ±2.2 kN, sensitivity 2.20 mV/N
Coaxial cable with BNC plugs	1	15 m
PCB Piezotronics 393B05 single-axis ceramic shear accelerometer	15	Range ±0.5 g, sensitivity ~10 V/g, Mass ≈ 120 g incl. MS base and magnet
MS flat bar	15	25 × 25 × 4.0
N42 rare earth disk magnets	15	20 dia. × 4.0
Coaxial cable with 10–32 sockets and BNC plugs	15	15 m
PCB Piezotronics 393B12 single-axis ceramic shear accelerometer	4	Range ±0.5 g, sensitivity ~10 V/g, Mass ≈ 340 g incl. MS base and magnet
MS flat bar	4	40 × 40 × 6.0
N42 rare earth ring magnets	4	25 dia. × 8.0
Coaxial cable with MILC-5015 sockets and BNC plugs	4	15 m
National instruments compact data acquisition system NI cDAQ-9172	1	Houses up to 8 modules
National instruments module NI 9234	5	Accepts up to 4 channels

Notes MS mild steel

18.3.4 Analysis and Results

The raw input data (impact hammer) were trimmed to 20 s time windows (102,400 data points) and truncated to reduce the influence of noise (see Fig. 18.2).

The raw response data were also trimmed to 20 s and de-trended. Minor adjustments were made to the data to account for sensors that were out of plumb and/or offset from a node point in order to create a 'virtual' signal at that node point.

Figure 18.3 shows ten repeated 'virtual' signals collected from one sensor during an impact test. The signals are well correlated, demonstrating the repeatability of the test method, which is one of the three key assumptions of modal analysis [6].

The auto spectra of the truncated impact force signal, $\boldsymbol{S_{ff}(\omega)}$, and normalized response signals, $\boldsymbol{S_{aa}(\omega)}$, were calculated using the *pwelch* function in MATLAB [5]. The cross-spectra, $\boldsymbol{S_{af}(\omega)}$ and $\boldsymbol{S_{fa}(\omega)}$, were calculated using the *cpsd* function in MATLAB [5]. The frequency response function (FRF) estimates, $\boldsymbol{H_1(\omega)}$ and $\boldsymbol{H_2(\omega)}$, were calculated using Eqs. 18.1 and 18.2 below:

$$\boldsymbol{H_1(\omega)} = \frac{\boldsymbol{S_{fa}(\omega)}}{\boldsymbol{S_{ff}(\omega)}} \tag{18.1}$$

$$\boldsymbol{H_2(\omega)} = \frac{\boldsymbol{S_{aa}(\omega)}}{\boldsymbol{S_{af}(\omega)}} \tag{18.2}$$

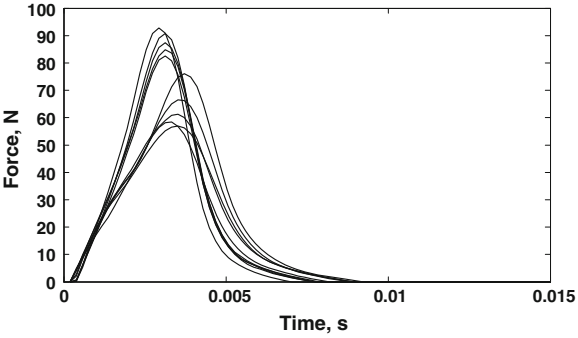

Fig. 18.2 Ten repeat truncated impact signals for one impact test

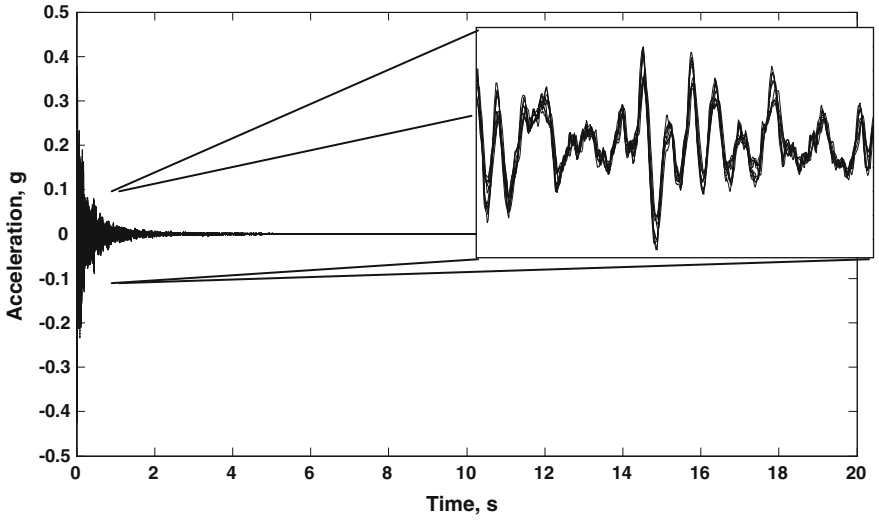

Fig. 18.3 Ten repeat acceleration signals from one sensor for one impact test (zoomed insert shows 0.1 s of data)

The coherence functions, γ^2, were also calculated using Eq. 18.3 below:

$$\gamma^2(\omega) = \frac{\boldsymbol{H}_1(\omega)}{\boldsymbol{H}_2(\omega)} \tag{18.3}$$

Figure 18.4 overleaf shows the log modulus (power, dB) plot of ten repeat $\boldsymbol{H}_2$ FRF estimates representing one impact test with one input location and one output location. These estimates are very well correlated, indicating a high degree of linearity in the structure, which is the most important of the three key assumptions for modal analysis [6].

The mean value of the repeat FRF estimates from each impact test was calculated and passed into a 300 × 300 FRF matrix. Each of the rows of the FRF matrix represents an output signal at a particular translational DOF and each of the columns represents an input signal at a particular translational DOF. For example, $\boldsymbol{H_{jk}}$ would denote the FRF for the $\boldsymbol{j}$th row and the $\boldsymbol{k}$th column. The diagonal FRFs of this matrix represent the driving point FRFs (i.e., where $\boldsymbol{j} = \boldsymbol{k}$). The remaining FRFs each have a reciprocal FRF (i.e., $\boldsymbol{H_{jk}}$ and $\boldsymbol{H_{kj}}$). Figure 18.5 on the next page shows a reciprocal pair of averaged $\boldsymbol{H}_1$ FRF estimates (DOF 145 and DOF 298). The two FRFs are well correlated for most of the resonance peaks which shows that the key assumption of reciprocity [6] holds true for this structure.

One of the simplest methods of identifying modes is to use a simple mode indicator function (MIF). The simplest MIF is found by summing all the absolute values of the FRFs in the FRF matrix. The premise of this method is that global resonance peaks will become more prominent in the MIF, whereas noise and local resonances will become less prominent. A variation of this MIF was adopted for this study whereby FRFs were grouped into three categories and averaged, not summed. The three categories are namely those where the inputs and outputs were both aligned in the: (1) global x direction (longitudinal), (2) global y direction (vertical), and (3) global z direction (lateral). Not only does this MIF highlight global resonance peaks, it also provides more insight into the mode shapes (i.e., whether they might be lateral, vertical, longitudinal, or a mixture). Figure 18.6 shows the directional MIF for this structure, representing the averages of 584 FRFs out of a possible 1,836. It can be observed that the first three modes are dominant, well separated, and have more power in the global z direction (lateral).

The frequencies and damping values of the first three modes were determined by applying the peak picking and half-power methods [6] to each FRF individually. Not all FRFs were useful in estimating these values, particularly at DOFs where the mode shape of interest was small in magnitude. Subsequently, the results from some FRFs were rejected. Results are presented in Table 18.2.

The experimental results for natural frequency showed very little variation, particularly for modes 1 and 2. This provides a great deal of confidence in the accuracy of frequency results.

There was more variation in the results for damping; however, it should be noted that other methods of modal analysis have been applied to the same structure with "*almost no agreement between the identified damping ratios from the two techniques*" of enhanced frequency-domain decomposition (EFDD) and data-driven stochastic subspace identification (SSI-DATA) [3] (p. 155). This suggests that it may not be possible to obtain accurate results for damping. Notwithstanding the lack of accuracy in damping results, it can be observed that modes 1 and 2 are lightly damped (approximately 0.7 %) and mode 3 is moderately damped (approximately 1.5 %).

The dynamic analysis of the numerical model produced mode shapes similar to those obtained experimentally, and in the same order as the experimentally obtained modes, however, the natural frequencies of the numerical model are significantly higher than those obtained experimentally.

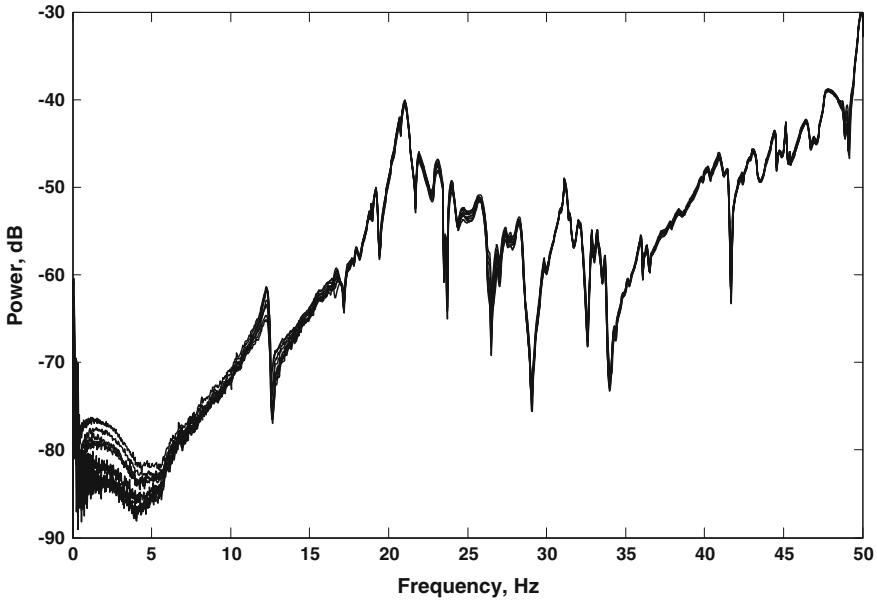

Fig. 18.4 Ten repeat $\boldsymbol{H}_2$ estimates from one sensor for one impact test

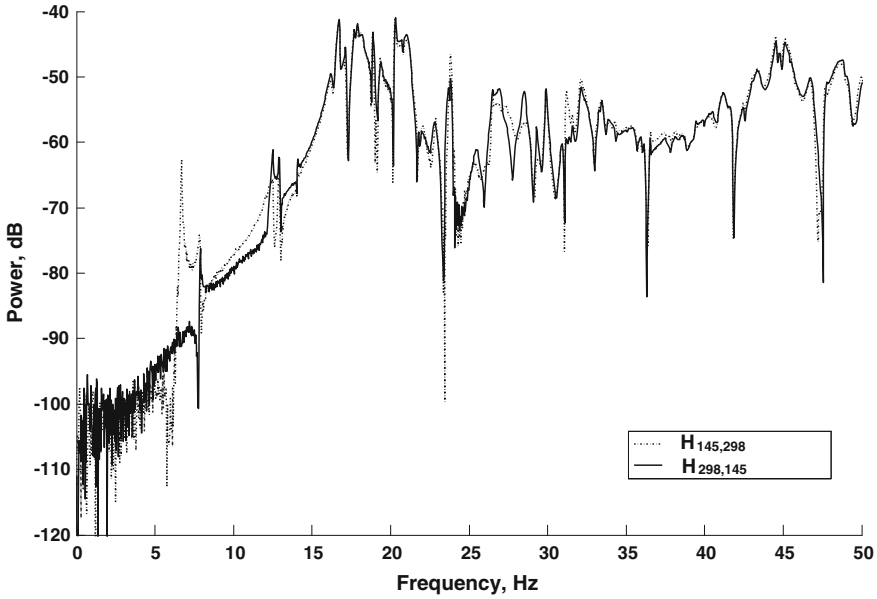

Fig. 18.5 Reciprocal pair of averaged $\boldsymbol{H}_1$ estimates for DOF 145 and DOF 298

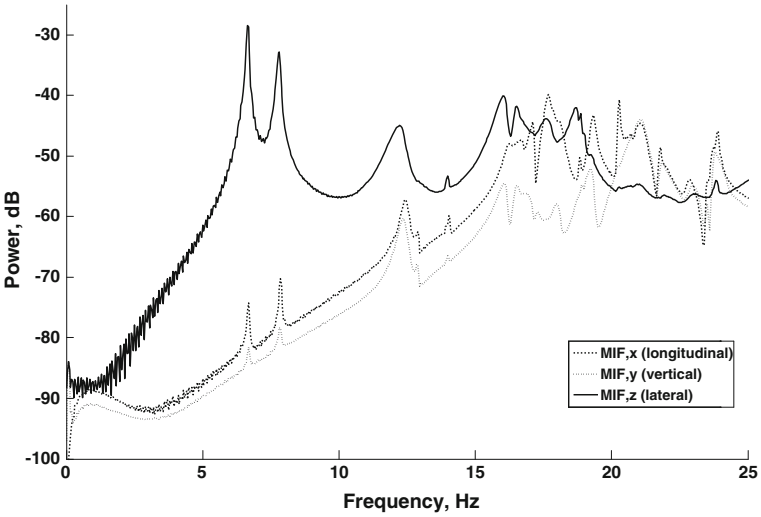

Fig. 18.6 Directional MIF

Table 18.2 Natural frequencies and damping of the first three modes

Mode no.	Frequency, Hz			Damping, ζ		Description
	Experimental		Numerical model			
	Mean	Std		Mean (%)	Std (%)	
1	6.672	0.027	9.99	0.743	0.063	Lateral sway 1
2	7.834	0.034	22.09	0.740	0.077	Lateral sway 2
3	12.325	0.137	33.18	1.548	0.455	Lateral bending 1

The mode shapes were obtained by using the quadrature picking method outlined in [7]. Each FRF within the FRF matrix was individually examined in the vicinity of resonance for modes 1, 2, and 3 and the peak value of the imaginary component of the FRF was selected as the mode shape value. With a focus on the 18 partially completed rows of the FRF matrix, mode shape values were interpolated for blank columns using a simple geometric method. The completed rows were then normalized and examined for consistency. Rows that were located near node points of a particular mode shape tended to show a lower consistency and were removed from the analysis. The remaining rows of normalized mode shape values were averaged to produce a smoother mode shape. Figures 18.7, 18.8 and 18.9 show the normalized and averaged mode shapes for modes 1, 2, and 3.

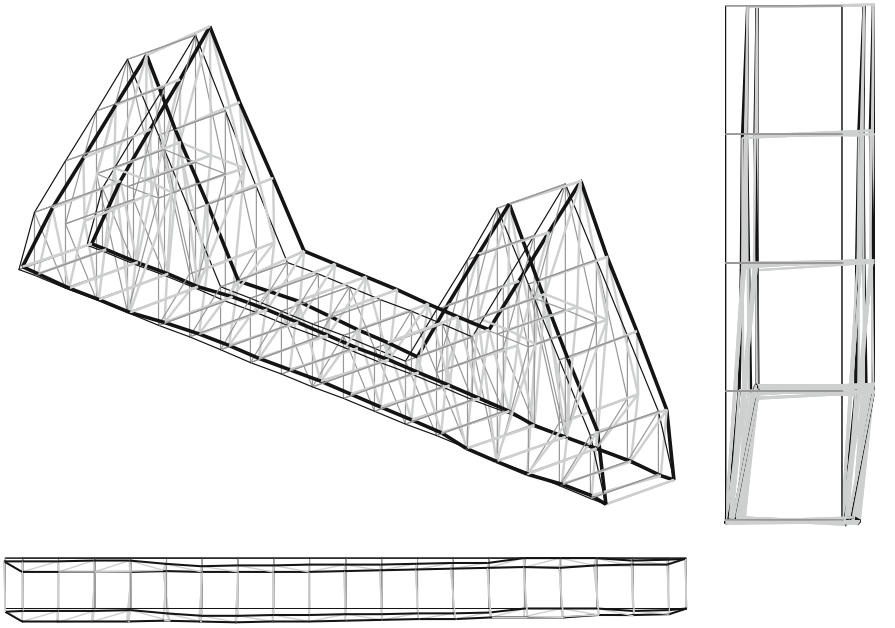

Fig. 18.7 Mode 1—Lateral sway 1, 6.67 Hz, 0.74 % damping

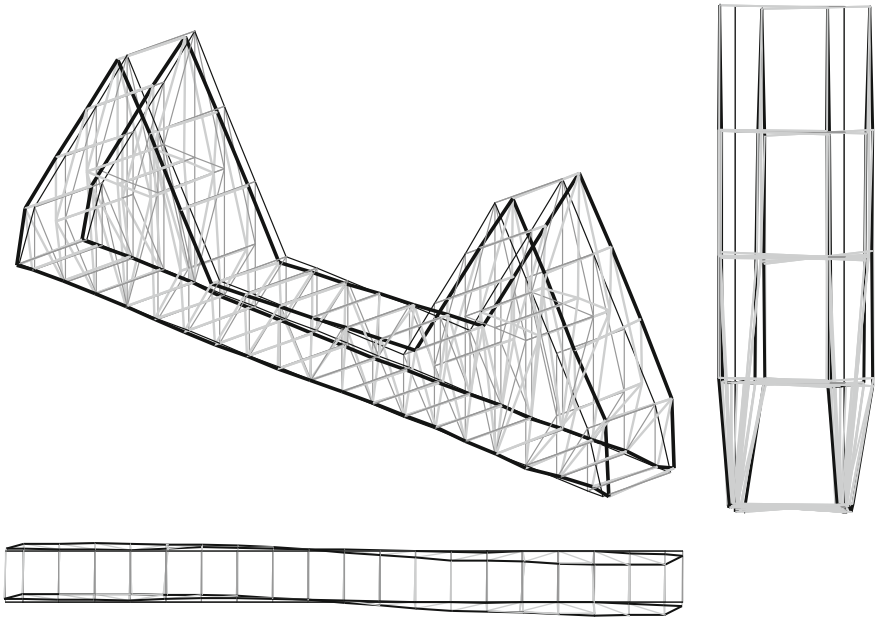

Fig. 18.8 Mode 2—Lateral sway 2, 7.83 Hz, 0.74 % damping

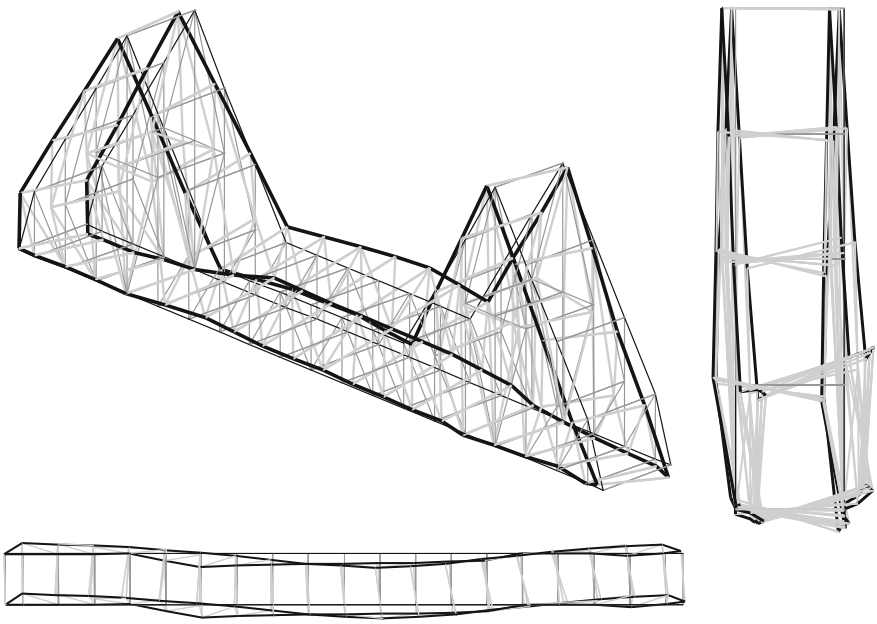

Fig. 18.9 Mode 3—Lateral bending 1, 12.33 Hz, 1.55 % damping

18.3.5 Discussion

The experimentally obtained frequencies did not match the results of the dynamic analysis of the numerical model; however, the order and shapes of the first three modes did match those of the numerical model. It should be noted that the boundary conditions of the numerical model were simplified as pins and rollers for the purpose of determining the design actions of the structure. These boundary conditions do not adequately represent the actual boundary conditions and consequently make the numerical model a lot stiffer than the actual structure. The numerical model will be updated as future work.

18.4 Conclusion

This paper has presented the preliminary modal testing and analysis of the bridge model which was described in the companion paper [1]. The aim of the experiment was presented. The equipment was listed, and the test method was detailed. The data were analyzed, and results were presented and discussed.

This experiment aimed to identify modal information of the first few modes of vibration, using impact hammer tests, and compare these results with the

numerical model of the structure. Modal information was obtained for the first three modes of vibration.

The mode shapes correlated well with those of the numerical model. The order of the modes obtained experimentally and numerically were the same; however, there was a significant difference between the frequencies of the experimentally obtained modes and those from the numerical model, which indicates that the numerical model needs refining. Experimentally obtained damping results were somewhat variable.

Acknowledgments This paper was developed within the CRC for Infrastructure and Engineering Asset Management, established and supported under the Australian Government's Cooperative Research Centres Programme. The primary author is a postgraduate student, studying at Queensland University of Technology, Brisbane. The primary author wishes to acknowledge the Australian Research Council for providing a living allowance scholarship, and the Cooperative Research Centre for Integrated Engineering Asset Management, Queensland Department of Transport and Main Roads and Brisbane City Council for providing top-up scholarships. Taringa Steel Pty. Ltd. are also acknowledged for their high quality craftsmanship in the fabrication of the bridge model.

References

1. Cowled CJL, Thambiratnam DP, Chan THT, Tan ACC (2012) Structural complexity in structural health monitoring: design of laboratory model and test plan. Paper presented at the 7th world congress on engineering asset management, Daejeon, Korea, 8–10 Oct 2012
2. Engineering Systems Pty Ltd (2010) Microstran v.8.11.100930 (software). Engineering Systems, Turramurra
3. Wang L (2012) Innovative damage assessment of steel truss bridges using modal strain energy correlation. Dissertation, Queensland University of Technology
4. National Instruments Corporation (2011) LabVIEW Signal Express 2011 v.5.0.0 (software). National Instruments Corporation, Austin, Texas
5. The Mathworks Inc (2012) MatLab R2012a (7.14.0.739) (software). The Mathworks Inc, Natick, Massachusetts
6. He J, Fu Z-F (2001) Modal analysis. Butterworth–Heinemann, Oxford
7. Agilent Technologies Inc (1997) The fundamentals of modal testing (Application Note 243-3). Agilent Technologies, Santa Clara, California